

Quantum Virial Coefficients via Path Integral Monte Carlo: Theory and Development of Novel Algorithms

PhD dissertation defense by: Ramachandran Subramanian

Committee: Prof. David A. Kofke (Chair),
Prof. Jeffrey R. Errington, Prof. Johannes Hachmann, Dr. Andrew J. Schultz

May 9, 2016

Overview

- 1 Introduction
 - Viral coefficients
 - *Ab initio* potentials
- 2 Objectives
- 3 Methods
 - Mayer Sampling Monte Carlo
 - Path Integral Monte Carlo
 - Novel algorithms
- 4 Results
 - Hydrogen
- 5 Summary

Virial equation of state (VEOS)

$$\frac{P}{\rho k T} = 1 + B_2(T)\rho + B_3(T)\rho^2 + \dots$$

- B_n - n^{th} order virial coefficient represents the effect of interaction of n molecules.
- Depends only on temperature.
- Works well for systems with low density (typically gases).

Expressions for the virial coefficients

- Second and third order virial coefficients are given by:

$$\begin{aligned} B_2(T) &= -\frac{1}{2} \int d1 f(0, 1) \\ B_3(T) &= -\frac{1}{3} \int \int d1 d2 f(0, 1) f(0, 2) f(1, 2) \end{aligned} \quad (1)$$

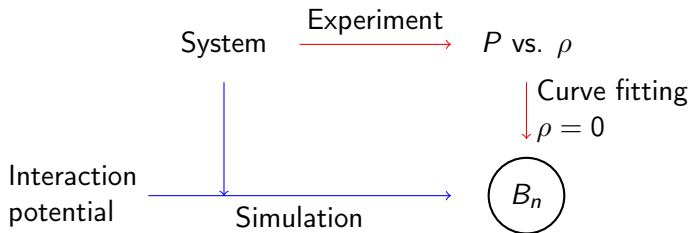
where $f(0, 1) = \left(\exp [- \beta U_2(\mathbf{r})] - 1 \right)$ and indices '1' and '2' denote the position and orientational degrees of freedom of molecules 1 and 2, respectively, with respect to molecule '0' at the origin.

- The number of such integrals to be summed¹ is: 3 for B_4 , 10 for B_5 , 56 for B_6 , 468 for B_7 .

¹ J. P. Hansen and I. R. McDonald, *Theory of Simple Liquids* (2006).

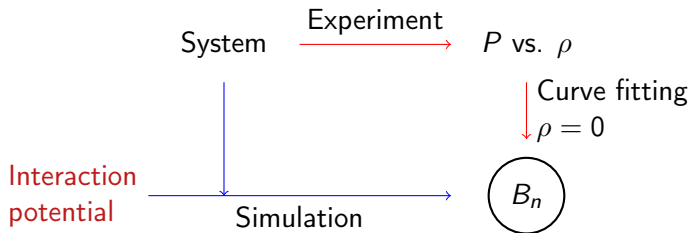
Main uses:

- To compute other thermodynamic properties like the joules-thomson coefficient, critical point etc.
- To rank different potential models by comparing their virial coefficients to experimental results



Main uses:

- To compute other thermodynamic properties like the joules-thomson coefficient, critical point etc.
- To rank different potential models by comparing their virial coefficients to experimental results



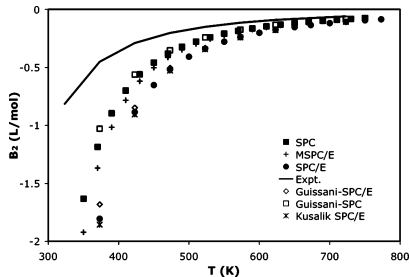
- To systematically tune and improve potentials as a result.

Empirical potential models

- Usually functions fitted to experimental data of bulk property measurement.
- Represent the net effect of a variety of phenomenon taking place including 2 body interactions, multi-body interactions, nuclear quantum effects etc.
- As a result, fail to accurately represent interaction potential.
- Interaction potentials that better represent condensed (high density) phase fail to predict accurate virial coefficients for the gas (low density) phase.

Example - different empirical models of water

- Importance of the accuracy of interaction potential²:



² K. M. Benjamin et al., J. Phys. Chem. B (2007).

Ab initio potential models

- Fundamentally different from empirical models as they focus only on two or three molecules at a time
- Solve for the interaction energies starting with the Schrödinger equation and involve many approximations:

$$\mathcal{H} \Psi = E \Psi,$$

$$\mathcal{H} = \mathcal{T}_e + \mathcal{T}_N + \mathcal{V}_{ee} + \mathcal{V}_{eN} + \mathcal{V}_{NN}$$

- Account for electronic structure using different levels of theory and different basis sets
- We use potentials fitted to *ab initio* data rather than compute it on-the-fly (expensive)

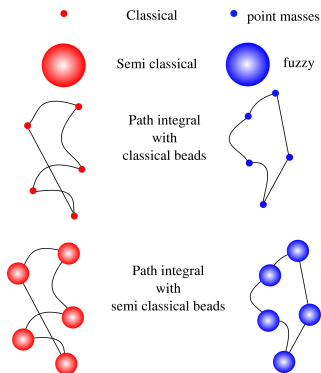
Nuclear quantum effects

- Consequence of uncertainty in the positions of atoms at low temperatures (Zero-point vibrational energy).
- Have to be explicitly included in virial coefficient calculations as they are ignored in the development of *ab initio* potentials.
- Semi-classical routes to include quantum effects:
 1. Computing first order quantum corrections.
 2. Using an effective potential like the Quadratic Feynman-Hibbs³.
- Quantum route: path integral Monte Carlo (PIMC) (will be explained in detail later).

³ R. P. Feynman and A. R. Hibbs, *Quantum Mechanics and Path Integrals* (1965).

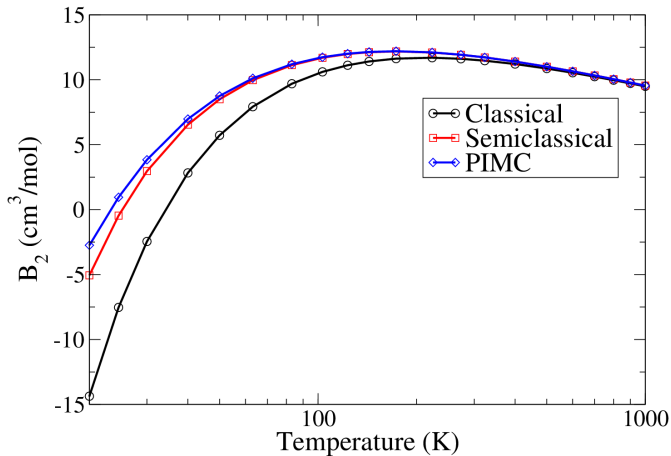
Classification of virial coefficients

- Different levels of “quantumness”, using B_2 as an example:



Nuclear quantum effects

- Importance of nuclear quantum effects⁴



⁴ K. R. S. Shaul, A. J. Schultz, and D. A. Kofke, J. Chem. Phys. (2012).

Overview

- 1 Introduction
 - Viral coefficients
 - *Ab initio* potentials
- 2 Objectives
- 3 Methods
 - Mayer Sampling Monte Carlo
 - Path Integral Monte Carlo
 - Novel algorithms
- 4 Results
 - Hydrogen
- 5 Summary

Objective

Diatomic molecules

Compute accurate virial coefficients using state-of-the-art *ab initio* potentials and PIMC method.

Overview

- 1 Introduction
 - Viral coefficients
 - *Ab initio* potentials
- 2 Objectives
- 3 **Methods**
 - Mayer Sampling Monte Carlo
 - Path Integral Monte Carlo
 - Novel algorithms
- 4 Results
 - Hydrogen
- 5 Summary

Mayer Sampling Monte Carlo

- Second and third order virial coefficients are given by:

$$B_2(T) = -\frac{1}{2} \int d1 f(0,1)$$

$$B_3(T) = -\frac{1}{3} \int \int d1 d2 f(0,1) f(0,2) f(1,2)$$

- MSMC⁵ is a free energy perturbation technique to evaluate the integrals in the above equations indirectly.

$$\Gamma(T) = \Gamma_o \frac{\langle \gamma/\pi \rangle_\pi / \langle \gamma_{os}/\pi \rangle_\pi}{\langle \gamma_o/\pi \rangle_{\pi_o} / \langle \gamma_{os}/\pi_o \rangle_{\pi_o}}$$

$$\gamma_{os} = \frac{|\gamma_o||\gamma|}{\alpha|\gamma_o| + |\gamma|}$$

⁵ J. K. Singh and D. A. Kofke, Phys. Rev. Lett. (2004).

PIMC - thermal density matrix

- The partition function is an important property in statistical mechanics:

$$P(x) = \frac{1}{Z} \rho(x, x),$$
$$Z = \int \rho(x, x) dx \equiv \text{trace}\{\rho\}.$$

where $\rho(x', x)$ is the statistical thermal density matrix at temperature T .

- Richard Feynman⁶ was able to connect it with quantum mechanics:

$$\rho(R, R'; \beta) = \langle R | e^{-\beta \mathcal{H}} | R' \rangle$$

where $R = \{\mathbf{r}_1, \mathbf{r}_2, \dots, \mathbf{r}_n\}$ and $\beta = 1/k_B T$, with k_B Boltzmann's constant and T the temperature.

⁶ R. P. Feynman and A. R. Hibbs, *Quantum Mechanics and Path Integrals* (1965).

Important equations

- A key property of the density matrix is that the product of two density matrices is also a density matrix. Hence the convolution⁷:

$$\rho(R_1, R_3; \beta_1 + \beta_2) = \int dR_2 \rho(R_1, R_2; \beta_1) \rho(R_2, R_3; \beta_2)$$

⁷ D. M. Ceperley, Rev. Mod. Phys. (1995).

⁸ T. Cui et al., Phys. Rev. B (1997).

Important equations

- A key property of the density matrix is that the product of two density matrices is also a density matrix. Hence the convolution⁷:

$$\rho(R_1, R_3; \beta_1 + \beta_2) = \int dR_2 \rho(R_1, R_2; \beta_1) \rho(R_2, R_3; \beta_2)$$

- As $\frac{\beta}{P} \rightarrow 0$ or equivalently as $PT \rightarrow \infty$, the “primitive approximation” is given by⁸:

$$e^{-\frac{\beta}{P}(\mathcal{T}+\mathcal{V})} \approx e^{-\frac{\beta}{P}\mathcal{T}} e^{-\frac{\beta}{P}\mathcal{V}}$$

⁷ D. M. Ceperley, Rev. Mod. Phys. (1995).

⁸ T. Cui et al., Phys. Rev. B (1997).

Important equations

- A key property of the density matrix is that the product of two density matrices is also a density matrix. Hence the convolution⁷:

$$\rho(R_1, R_3; \beta_1 + \beta_2) = \int dR_2 \rho(R_1, R_2; \beta_1) \rho(R_2, R_3; \beta_2)$$

- As $\frac{\beta}{P} \rightarrow 0$ or equivalently as $PT \rightarrow \infty$, the “primitive approximation” is given by⁸:

$$e^{-\frac{\beta}{P}(\mathcal{T}+\mathcal{V})} \approx e^{-\frac{\beta}{P}\mathcal{T}} e^{-\frac{\beta}{P}\mathcal{V}}$$

- The Trotter formula proves that this approximation does converge to the right result in the $P \rightarrow \infty$ limit and is given by:

$$e^{-\beta(\mathcal{T}+\mathcal{V})} = \lim_{P \rightarrow \infty} \left[e^{-\frac{\beta}{P}\mathcal{T}} e^{-\frac{\beta}{P}\mathcal{V}} \right]^P$$

⁷ D. M. Ceperley, Rev. Mod. Phys. (1995).

⁸ T. Cui et al., Phys. Rev. B (1997).

Diatomic molecule - rigid rotor⁹

- Let m and I denote the mass of the atom and moment of inertia of the rigid rotor respectively with $\Lambda_m = h/\sqrt{2\pi m k_B T}$. Its Hamiltonian is given by:

$$\hat{h}_2 = \frac{\hat{\mathbf{p}}^2}{2m} + \frac{\hat{\mathbf{J}}_1^2}{2I} + \frac{\hat{\mathbf{J}}_2^2}{2I} + \hat{U}(r, \Omega_1, \Omega_2)$$

where $\hat{\mathbf{p}}$ is the momentum operator conjugated to the COM separation, $\hat{\mathbf{J}}_1$ and $\hat{\mathbf{J}}_2$ are the angular momentum operators, $\hat{U}(r, \Omega_1, \Omega_2)$ is the intermolecular potential function in terms of the COM distance r and the orientation vectors Ω_1 and Ω_2 .

⁹ K. Patkowski et al., J. Chem. Phys. (2008).

Diatomic molecule - rigid rotor¹⁰

- Use $\mathbf{x}^i, \Omega_1^i, \Omega_2^i$ to denote the configuration of the i^{th} rigid rotors,

Matrix elements

$$\begin{aligned}\mathcal{T}_{\text{tra}}^{i,i+1} &= \left\langle \mathbf{x}^i \left| \exp \left(-\frac{\beta \hat{\mathbf{p}}^2}{2mP} \right) \right| \mathbf{x}^{i+1} \right\rangle = \frac{P^{3/2}}{\Lambda_m^3} \exp \left(-\frac{\pi P (\mathbf{x}^i - \mathbf{x}^{i+1})^2}{\Lambda_m^2} \right) \\ \mathcal{T}_{\text{rot}}^{i,i+1} &= \left\langle \Omega^i \left| \exp \left(-\frac{\beta \hat{\mathbf{J}}^2}{2IP} \right) \right| \Omega^{i+1} \right\rangle = \sum_{j=0}^{\infty} \frac{2j+1}{4\pi} \mathcal{P}_j(\cos(\theta_{i,i+1})) \\ &\quad \times \exp[-\beta j(j+1)\Upsilon/P]\end{aligned}$$

where j is the angular quantum number, $\theta_{i,i+1}$ is the angle between bead orientation vectors Ω_i, Ω_{i+1} , \mathcal{P}_j is the Legendre polynomial of order j and $\Upsilon = \hbar^2/(2I)$.

¹⁰ K. Patkowski et al., J. Chem. Phys. (2008).

Diatomic molecule - rigid rotor¹⁰

- Use $\mathbf{x}^i, \Omega_1^i, \Omega_2^i$ to denote the configuration of the i^{th} rigid rotors,

Matrix elements

$$\begin{aligned}\mathcal{T}_{\text{tra}}^{i,i+1} &= \left\langle \mathbf{x}^i \left| \exp \left(-\frac{\beta \hat{\mathbf{p}}^2}{2mP} \right) \right| \mathbf{x}^{i+1} \right\rangle = \frac{P^{3/2}}{\Lambda_m^3} \exp \left(-\frac{\pi P (\mathbf{x}^i - \mathbf{x}^{i+1})^2}{\Lambda_m^2} \right) \\ \mathcal{T}_{\text{rot}}^{i,i+1} &= \left\langle \Omega^i \left| \exp \left(-\frac{\beta \hat{\mathbf{J}}^2}{2IP} \right) \right| \Omega^{i+1} \right\rangle = \sum_{j=0}^{\infty} \frac{2j+1}{4\pi} \mathcal{P}_j(\cos(\theta_{i,i+1})) \\ &\quad \times \exp[-\beta j(j+1)\Upsilon/P]\end{aligned}$$

where j is the angular quantum number, $\theta_{i,i+1}$ is the angle between bead orientation vectors Ω_i, Ω_{i+1} , \mathcal{P}_j is the Legendre polynomial of order j and $\Upsilon = \hbar^2/(2I)$.

¹⁰ K. Patkowski et al., J. Chem. Phys. (2008).

Diatomic molecule - rigid rotor¹⁰

- Use $\mathbf{x}^i, \Omega_1^i, \Omega_2^i$ to denote the configuration of the i^{th} rigid rotors,

Matrix elements

$$\begin{aligned}\mathcal{T}_{\text{tra}}^{i,i+1} &= \left\langle \mathbf{x}^i \left| \exp \left(-\frac{\beta \hat{\mathbf{p}}^2}{2mP} \right) \right| \mathbf{x}^{i+1} \right\rangle = \frac{P^{3/2}}{\Lambda_m^3} \exp \left(-\frac{\pi P (\mathbf{x}^i - \mathbf{x}^{i+1})^2}{\Lambda_m^2} \right) \\ \mathcal{T}_{\text{rot}}^{i,i+1} &= \left\langle \Omega^i \left| \exp \left(-\frac{\beta \hat{\mathbf{J}}^2}{2IP} \right) \right| \Omega^{i+1} \right\rangle = \sum_{j=0}^{\infty} \frac{2j+1}{4\pi} \mathcal{P}_j(\cos(\theta_{i,i+1})) \\ &\quad \times \exp[-\beta j(j+1)\Upsilon/P]\end{aligned}$$

where j is the angular quantum number, $\theta_{i,i+1}$ is the angle between bead orientation vectors Ω_i, Ω_{i+1} , \mathcal{P}_j is the Legendre polynomial of order j and $\Upsilon = \hbar^2/(2I)$.

¹⁰ K. Patkowski et al., J. Chem. Phys. (2008).

Diatomic molecule - rigid rotor¹¹

- Defining $\mathbf{r} \equiv \mathbf{x}^{(1)}$, $\Delta^{(i)} \equiv \mathbf{x}^{(i+1)} - \mathbf{x}^{(i)}$,

$$\exp[-\beta \bar{U}(|\mathbf{r}|)] = \left\langle \exp \left[-\frac{\beta}{P} \sum_{i=1}^P U(|\mathbf{x}^i|, \Omega_1^i, \Omega_2^i) \right] \right\rangle_{F, \varrho}$$

- Probability distributions:

$$\varrho(\Omega) = \frac{1}{q_{\text{rot}}} \prod_{i=1}^P \mathcal{T}_{\text{rot}}^{i,i+1}, \quad F(\Delta) = \Lambda_m^3 \prod_{i=1}^P \mathcal{T}_{\text{tra}}^{i,i+1}$$

$$q_{\text{rot}} = \sum_{j'} (2j' + 1) \exp[-\beta \Upsilon j'(j' + 1)]$$

Fully quantum second virial coefficient

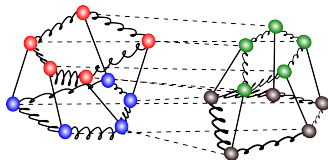
$$B_2(T) = -2\pi \int dr r^2 (e^{-\beta \bar{U}(r)} - 1)$$

¹¹ K. Patkowski et al., J. Chem. Phys. (2008).

Diatomic molecule - rigid rotor¹²

- A closer look at the effective potential:

$$\exp[-\beta \bar{U}(|\mathbf{r}|)] = \left\langle \exp \left[-\frac{\beta}{P} \sum_{i=1}^P U(|\mathbf{x}^i|, \Omega_1^i, \Omega_2^i) \right] \right\rangle_{F, \varrho}$$



¹² K. Patkowski et al., J. Chem. Phys. (2008).

Objectives

Diatomic molecules

Compute accurate virial coefficients using state-of-the-art *ab initio* potentials, MSMC and PIMC methods for the rigid case.

Challenges

Lack of efficient an sampling algorithm for orientations.

Orientation sampling

- Idea proposed by Garberoglio et al.¹³: two independent atoms (vs. one rigid rotor previously).
- Leads to possibility of avoiding quantum chemistry calculations.
- Sampling problem can be analyzed more mathematically, without having to worry about the physics of the rigid rotor.
- Straightforward but non-trivial extension to multiatomic systems.

¹³ G. Garberoglio et al., J. Chem. Phys. (2014).

Orientation sampling

- Instead of using Cartesian coordinates, we use the P COM position vectors \mathbf{R}_i and the P bead (or image) vectors \mathbf{b}_i .
- We consider both Boltzmann type as well as exchange type configurations.
- Probability associated with a configuration $\mathbf{Z} \equiv (\mathbf{R}, \mathbf{b})$ is given as:

$$P_{\sigma}(\mathbf{Z}) = \frac{1}{Q_1^{(\sigma)}} F(\mathbf{R}; 2m) F(\mathbf{b}^{(\sigma)}; m/2) e^{-\beta \bar{u}(\mathbf{b})}$$

where F is the path-integral weight, and \bar{u} is the intramolecular potential energy averaged over all images:

$$F(\mathbf{x}; m) = \left(\frac{P^{3/2}}{\Lambda_m^3} \right)^P \exp \left[-\frac{\pi P}{\Lambda_m^2} \sum_{i=0}^{P-1} |\mathbf{x}_{i+1} - \mathbf{x}_i|^2 \right]$$

$$\bar{u}(\mathbf{b}) = \frac{1}{P} \sum_{i=0}^{P-1} u(b_i)$$

Orientation sampling

- Define π to be the ***b***-dependent terms of the probability distribution F .
- We sample from an approximate distribution $\tau(o \rightarrow n)$ and accept or reject based on:

$$P_{\text{acc}} = \text{Min} \left[1, \frac{\pi(n)/\pi(o)}{\tau(o \rightarrow n)/\tau(n \rightarrow o)} \right]$$

where '*o*' and '*n*' denote the old and new configurations respectively.

- We derive a simple and analytic expression for $\tau(o \rightarrow n)$

Orientation sampling - bisection algorithm

- Angle between image 0 and image P is 0 for Boltzmann type and π for exchange type conformations. The choice of orientation of image 0 is arbitrary
- At every stage, we are given two images $\mathbf{b}_i, \mathbf{b}_k$ and we choose the orientation of image $j = (i + k)/2$.
- We note that $\tau(o \rightarrow n)$ is exact for the last step of the algorithm.



Figure 1: Example for $P = 8$

Orientation sampling - bisection algorithm

- Angle between image 0 and image P is 0 for Boltzmann type and π for exchange type conformations. The choice of orientation of image 0 is arbitrary
- At every stage, we are given two images $\mathbf{b}_i, \mathbf{b}_k$ and we choose the orientation of image $j = (i + k)/2$.
- We note that $\tau(o \rightarrow n)$ is exact for the last step of the algorithm.



Figure 1: Example for $P = 8$

Orientation sampling - bisection algorithm

- Angle between image 0 and image P is 0 for Boltzmann type and π for exchange type conformations. The choice of orientation of image 0 is arbitrary
- At every stage, we are given two images $\mathbf{b}_i, \mathbf{b}_k$ and we choose the orientation of image $j = (i + k)/2$.
- We note that $\tau(o \rightarrow n)$ is exact for the last step of the algorithm.

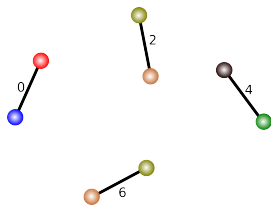


Figure 1: Example for $P = 8$

Orientation sampling - bisection algorithm

- Angle between image 0 and image P is 0 for Boltzmann type and π for exchange type conformations. The choice of orientation of image 0 is arbitrary
- At every stage, we are given two images $\mathbf{b}_i, \mathbf{b}_k$ and we choose the orientation of image $j = (i + k)/2$.
- We note that $\tau(o \rightarrow n)$ is exact for the last step of the algorithm.

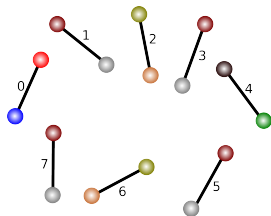


Figure 1: Example for $P = 8$

Orientation sampling

- Adjacent image probability distribution:

$$\begin{aligned}
 \tau^{\text{adj}}(\mathbf{b}_j(\alpha, \beta) : \mathbf{a}_j, \psi_{i,k}) \\
 &= \pi(\mathbf{b}_i, \mathbf{b}_j) \pi(\mathbf{b}_j, \mathbf{b}_k) \\
 &= \exp(-4k_h[d_{AC}^2 + d_{BC}^2]/b^2) \\
 &= \exp(-4k_h[1 - \cos(\psi_{i,k}/2) \cos(\alpha)])
 \end{aligned}$$

- The angle α can be calculated by choosing C at random, uniformly on $[0, 1]$.

$$\begin{aligned}
 \alpha &= \cos^{-1} \left[1 + (1/\kappa) \right. \\
 &\quad \left. \times \ln(1 - C(1 - \exp[-2\kappa])) \right], \\
 \kappa &= 4 \cos(\psi_{i,k}/2) k_h b^2
 \end{aligned}$$

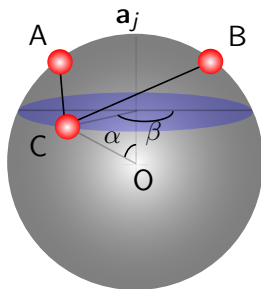


Figure 2: Simplified picture

Objectives

Diatomic molecules

Compute accurate virial coefficients using state-of-the-art *ab initio* potentials, MSMC and PIMC methods for the flexible case.

Challenges

To include vibrational degrees of freedom.

Methods to handle flexibility

- Instead of using ground state bond length (r_0) use average bond length at each temperature ($\langle r \rangle_T$)¹⁴
- Average the entire intermolecular potential ($\langle U \rangle_T$) over internal degrees of freedom of each monomer, weighted by the appropriate wave function¹⁵:

$$\langle r \rangle_T = \sum_{n,J} p(n, J : T) \langle \chi_{nJ} | r | \chi_{nJ} \rangle$$

where n and J are rotational and vibrational quantum numbers respectively, while χ_{nJ} denotes the corresponding wave-function.

$$p(n, J : T) = \frac{(2J + 1) \exp(-E(n, J)/T)}{\sum_{n', J'} (2J' + 1) \exp(-E(n', J')/T)}$$

where $E(n', J')$ is the energy of the (n', J') state.

¹⁴ G. Garberoglio et al., J. Chem. Phys. (2012).

¹⁵ G. Garberoglio et al., J. Chem. Phys. (2014).

Bond-length sampling

- Define π in a similar fashion to the orientation sampling algorithm:

$$\pi(\mathbf{b}) = \prod_{i=0}^{P-1} b_i^2 e^{-\beta u(b_i)/P} \pi(b_i, b_{i+1}, \theta_{i,i+1})$$

$$\pi(b_i, b_j, \theta_{i,j}) = \exp\left(-\frac{1}{2}k_h(b_i^2 + b_j^2 - 2b_i b_j \cos(\theta_{i,j}))\right)$$

where $\theta_{i,j}$ is the angle between orientations of images i and j .

Bond-length sampling

- Let $\pi(\mathbf{b}) = \exp(-y)$, where y can be defined as follows:-

$$y = \sum_{i=0}^{P-1} \left\{ k_h \left(b_i^2 - b_i b_j \cos(\theta_{ij}) \right) - 2 \log b_i + \frac{\beta u(b_i)}{P} \right\}$$

- We define $\tilde{y} \approx y$ such that:

$$\tilde{y} = \sum_{i=0}^{P-1} \left\{ k_h \left(b_i^2 - b_i b_j \right) - \frac{2 \log b_i}{P} + \frac{\beta u(b_i)}{P} \right\}$$

- We solve for the nominal $\cos(\hat{\theta})$ value by:

$$\frac{\partial y}{\partial b_i} = \frac{\partial \tilde{y}}{\partial b_i} \Rightarrow \cos(\hat{\theta}) = 1 - \frac{P-1}{P k_h b_i^2}$$

- Using this nominal value in the expression for y , we find b_m such that:

$$\left. \frac{\partial y}{\partial b_i} \right|_{b_i=b_m} = 0 \quad \forall i$$

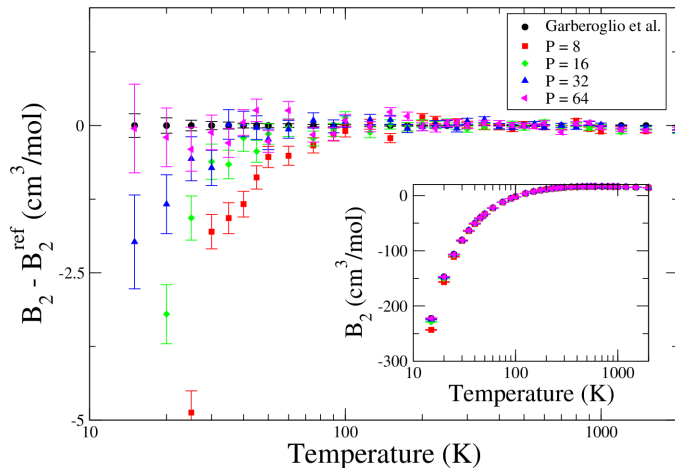
Overview

- 1 Introduction
 - Viral coefficients
 - *Ab initio* potentials
- 2 Objectives
- 3 Methods
 - Mayer Sampling Monte Carlo
 - Path Integral Monte Carlo
 - Novel algorithms
- 4 Results
 - Hydrogen
- 5 Summary

Computational details

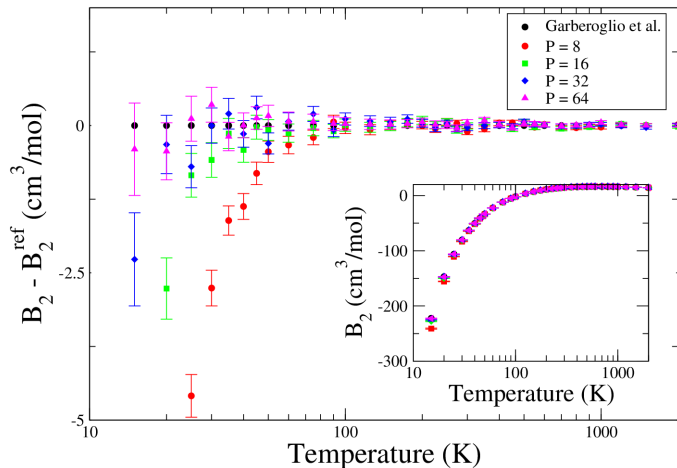
- A short equilibration simulation is performed at the beginning to determine α and to adjust MC move step sizes so that the acceptance of all the MC moves is 50%.
- Irrespective of their number, all MC moves are chosen with equal probability for both the systems within the simulation.
- The total number of configuration samples is divided into blocks of 1000 samples each. We compute averages across all blocks for the four ratios and use standard error propagation formulas to arrive at the final result.
- Error bars shown represent one standard deviation of the mean (68% confidence interval).

Bond length¹⁶ - $\langle r \rangle_0$ - 10^7 configuration samples total



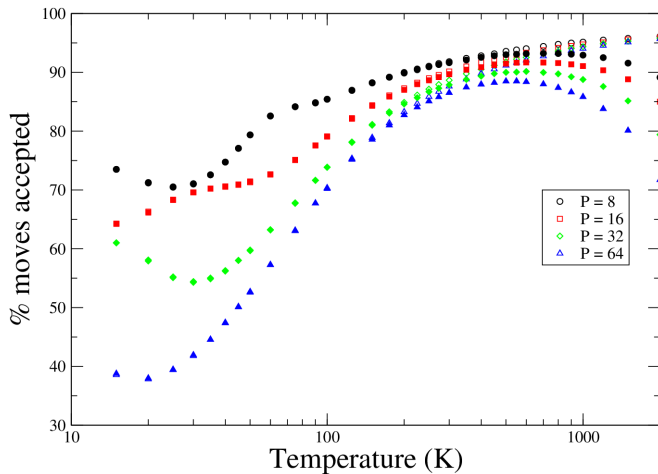
¹⁶ G. Garberoglio et al., J. Chem. Phys. (2014).

Bond length¹⁷- $\langle r \rangle_T - 10^7$ configuration samples total

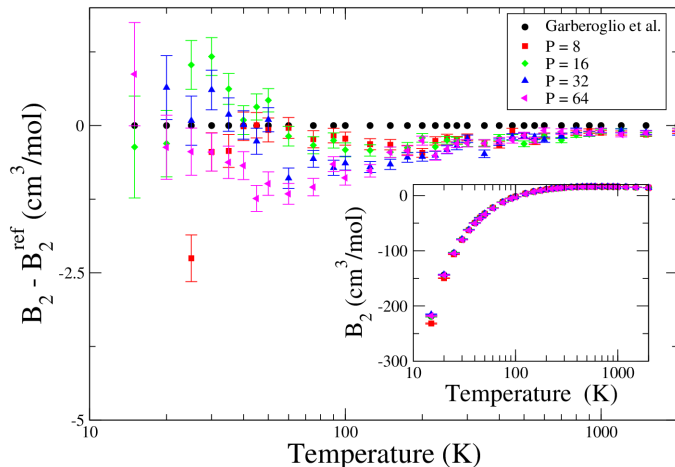


¹⁷ G. Garberoglio et al., J. Chem. Phys. (2014).

Performance of the orientation move

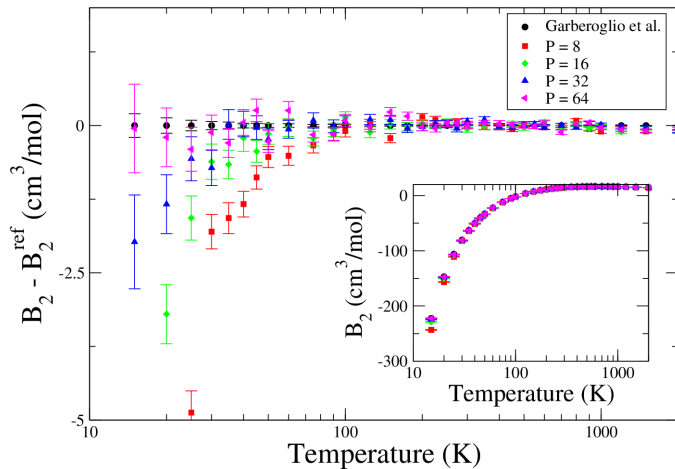


Bond length¹⁸- flexible bond-length - 10^7 configuration samples total



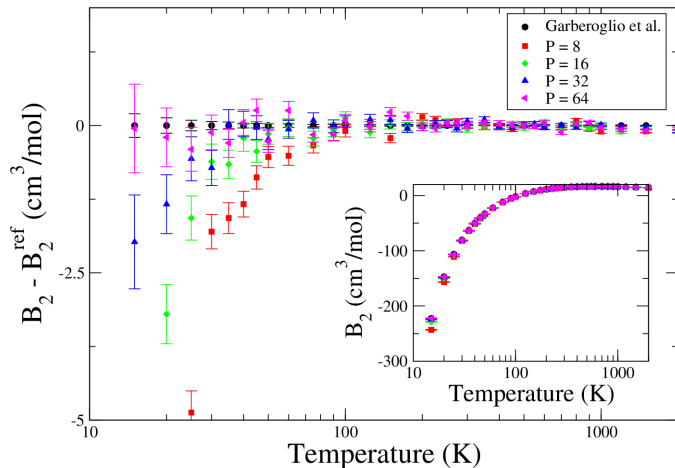
¹⁸ G. Garberoglio et al., J. Chem. Phys. (2014).

Bond length¹⁹ - $\langle r \rangle_0$



¹⁹ G. Garberoglio et al., J. Chem. Phys. (2014).

Bond length²⁰ - $\langle r \rangle_0$



²⁰ G. Garberoglio et al., J. Chem. Phys. (2014).

Overview

- 1 Introduction
 - Viral coefficients
 - *Ab initio* potentials
- 2 Objectives
- 3 Methods
 - Mayer Sampling Monte Carlo
 - Path Integral Monte Carlo
 - Novel algorithms
- 4 Results
 - Hydrogen
- 5 Summary